UNCORRECTED PROOFS

ANALYSIS OF THE NATURAL REMANENT MAGNETIZATION OF ROCKS BY MEASURING THE EFFICIENCY RATIO THROUGH ALTERNATING FIELD DEMAGNETIZATION SPECTRA

T. KOHOUT[1,2,3], G. KLETETSCHKA[3,4,5], F. DONADINI[1*], M. FULLER[6], E. HERRERO-BERVERA[6]

1 Department of Physical Sciences, University of Helsinki, P. O. Box 64, Helsinki, Finland (tomas.kohout@helsinki.fi)

2 Department of Applied Geophysics, Charles University, Albertov 6, 128 43 Praha 2, Czech Republic

3 Institute of Geology, Acad. Sci. Czech Republic, Rozvojová 269, 165 00 Praha 6, Czech Republic

4 Department of Physics, Catholic University of America, Washington D.C., USA

5 NASA Goddard Space Flight Center, Code 691, Greenbelt, Maryland, USA

6 HIGP-SOEST, University of Hawaii at Manoa, Honolulu, HI, 96822, USA

* Present Address: Inst. Geophys. Planet. Phys., 9500 Gilman Drive 0225, Univ. California, La Jolla, CA92093-0225, USA

Received: March 5, 2007; Revised: November 9, 2007, 2007; Accepted: February 18, 2008

ABSTRACT

The REM(AF) method is a new tool for the analysis of the origin and alternating field demagnetization coercivity spectra of the remanent magnetization. We applied this method on precambrian Gila diabase sheets from Arizona in order to identify the high coercivity magnetic carrier, and on artificially shocked Rowley Regis basalt from UK in order to analyze the effect of the shock on the natural remanent magnetization.

In the Gila diabase the high coercivity magnetic component was identified to be most likely represented by the acicular magnetite (increase in the efficiency ratio in the high coercivity region).

In the Rowley Regis basalt, the the REM(AF) analysis revealed that comparing to NRM the shock produced different distribution of the AF demagnetization coercivity spectra due to the occurrence of the Shock Remanent Magnetization.

The limitations of the method are the presence of multidirectional remanence components in the sample influencing the efficiency (REM) values. Also in the presence of hard coercivity minerals like hematite or pyrrhotite it is hard to reach complete saturation of the rock using common laboratory magnetizers, resulting in overestimated efficiency values in the high coercivity region.

Key words: *REM*, efficiency of magnetization, coercivity, shock remanence, *SRM*

© 2008 Inst. Geophys. AS CR, Prague

1. INTRODUCTION

A new method for Alternating Field (AF) demagnetization coercivity analysis of the remanent magnetization has been developed by *Kletetschka et al. (unpublished results)*. The method is a modification of the plots of Natural Remanent Magnetization (*NRM*) vs. Saturation Isothermal Remanent Magnetization (*SIRM*) introduced by *Jarrard and Cockerham (1975)*, and further developed by *Cisowski et al. (1986, 1990)* and *Fuller et al. (1988)*. This technique utilizes a detailed AF demagnetization of *NRM*, followed by AF demagnetization of the *SIRM* in the same AF field steps. Then the efficiency of the *REM* ratio, which is calculated as the *NRM*/*SIRM* ratio (*Wasilewski, 1977*) is determined for each demagnetization step and is plotted as a function of the AF demagnetization field (see Fig. 4 later). The *REM*(AF) method does not require any heating and thus the alteration of the samples due to the heating is prevented.

The resulting *REM*(AF) curve displays the magnetization efficiency ratio and its variations through the whole AF demagnetization coercivity region and yield useful information about the acquisition of the *NRM* in a rock sample. For example, the initial *REM* value (which equals the *NRM*/*SIRM* before demagnetizing) depends on the magnetizing paleofield as shown by *Fuller (1974)*, *Wasilewski (1977)*, *Cisowski and Fuller (1986)*, *Fuller et al. (1988)*, *Yu (2006)*, *Yu et al. (2007)* and also on the saturation magnetization (M_S) of the magnetic mineral (*Kletetschka et al., 2004*). Thus one of the applications of the *REM*(AF) method is the rough paleofield estimate.

Previous studies of the variation of the efficiency ratio during AF demagnetization were done mainly on magnetite bearing rocks (*Fuller et al., 1998*) and synthetic magnetite samples (*Yu, 2006*) The results of those studies indicate that slope of the *REM*(AF) curve contains information about the primary magnetizing process and secondary events (viscous overprint, alteration, shock effects). The *REM*(AF) curve of a thermoremanent magnetization (*TRM*) is roughly flat in the case of multidomain (MD) grains and slightly increasing towards higher demagnetizing AF peak fields in the case of single domain (SD) and pseudosingle domain (PSD) grains (*Yu, 2006*; *Fuller et al., 1988*). In this case the increase of the *REM*(AF) ratio through AF demagnetization due to the grain size effect is observed to be in the same order of magnitude, typically not exceeding double of the initial *REM* value. In contrast for the IRM type of magnetization, the negative slope of the *REM*(AF) curve is typical in the low AF demagnetization coercivity region due to relatively higher susceptibility of the lower coercivity grains to the IRM acquisition process (*Kletetschka et al., unpublished results*). For the same reason, the viscous effects (overprint, viscous relaxation) residing in the MD (Multidomain) grains influence the efficiency ratio in the low coercivity region as is indicated by the variation of the *REM*(AF) curve in the beginning of the AF demagnetization process (*Cisowski et al, 1990*; *Fuller et al, 1988*).

However, the correct estimate of the *REM* ratio depends also on the number and directions of the magnetic components within the rock specimen. For example, the *REM* value would be biased when the specimen contains *NRM* components that are not parallel due to addition of the magnetization vectors of various directions. It is also necessary to note that the *REM* ratio is sensitive to the effect of under-saturation of specimens (i.e. due to presence of fine grained high coercive magnetic minerals like hematite or pyrrhotite

failing to reach complete saturation even in fields of several Teslas) The *REM* values of the under-saturated rocks can be then overestimated and this trend is pronounced in the high coercivity (high AF) region.

We applied this method on precambrian Gila diabase sheets from Arizona and on artificially shocked Rowley Regis basalt in order to analyze the remanent magnetization of those rocks. In particular we were interested in investigating the magnetic carriers of the Arizona samples, and in analyzing the shock effect on the magnetization of the Rowley Regis Basalt.

2. INSTRUMENTS AND METHODS

2.1. Measurements of the Gila Diabase Sheets

The magnetic susceptibility measurements (susceptibility vs. temperature measurements) were done using a KLY-3S kappa-bridge (operating at 975 Hz frequency and 300 A/m RMS field intensity) equipped with temperature control units (CS-L and CS-3) at the Department of Physical Sciences, University of Helsinki (HU). For magnetic remanence measurements, the 2G Model 755 Superconducting Rock Magnetometer at HU was used in combination with the Applied Physics Model 2G600 AF demagnetizer. The AF demagnetization of remanent magnetization (*NRM* and *SIRM*) was always performed using the same procedure consisting of subsequent 3-axis demagnetization using 2G800 automatic sample handler for discrete sample measurements. The field steps, field ramp and hold time settings were constant for all experiments.

For hysteresis parameters measurements as well as for *SIRM* acquisition the Princeton Measurements Model 3900 VSM (Vibrating Sample Magnetometer) at HU was used (max. field 1 T). The *SIRM* was imprinted using electromagnet ramp up-down cycle with the field-overshoot prevention.

For the IRM acquisition the Magnetic Measurements MMPM10 pulse magnetizer at the Institute of Geology, Academy of the Sciences of the Czech Republic was used which is capable of generating pulse fields up to 3 T on standard paleomagnetic samples (cylinders 2.5 cm in diameter and height).

2.2. Measurements of the Rowley Regis Basalt

Measurements of the remanence of a control and shocked samples from the basalt were made on the 2G 750 with in line AF demagnetization at the University of California, Santa Barbara. Both *NRM* and *SIRM* were demagnetized along three perpendicular axes. The *SIRM* was produced using a 1 T field.

3. RESULTS

3.1. The Magnetomineralogy of the Precambrian Gila Diabase Sheets (Arizona, USA)

Eighty five samples from the 1.1 Ga old Gila diabase sheets from Arizona, USA (carrying *TRM*) were studied to investigate the origin of the asymmetric reversal observed

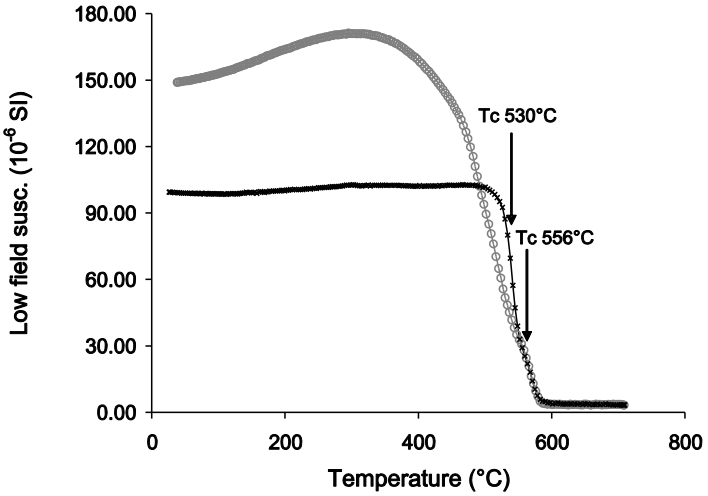

Fig. 1. Magnetic low-field susceptibility (unnormalized) vs. temperature plot (black crosses - heating; grey circles - cooling) of the Gila diabase sample. The heating curve reveals two populations of the titanomagnetite (Curie temperatures T_C 530°C and 556°C) to be present. Only the higher T_C phase is thermally stable (reversible on the cooling curve).

in Laurentia around that period (*Donadini et al., unpublished results*). For this study, five specimens were selected and studied with the *REM*(AF) method.

The thermomagnetic curve shows in general two populations of the titanomagnetite (Curie temperatures T_C of 530°C and 556°C) to be present in the samples (Fig. 1). The hysteresis parameters plotted in the Day plot reveal mostly MD-SD or SP-SD like (SP - Super-Paramagnetic) behavior (Fig. 2).

Fig. 3 shows an example of the AF demagnetization characteristics of the sample labeled FD1-2b. The characterization of the FD1-2b sample is similar to the other four samples studied and thus the figures only for the FD1-2b sample are presented. From the Zijderveld demagnetization diagram three *NRM* components can be identified. The low coercivity component (20% of the absolute *NRM* value) residing in the MD magnetite grains is removed by 10 mT AF field. The intermediate coercivity component (50% of the absolute *NRM* value) is stable in the 10 – 25 mT AF field region. The remaining 30% of the *NRM* (the high coercivity component) is magnetically hard. Even at the maximum applied AF field (160 mT) 5% of the *NRM* is preserved and directionally stable. The residual moment of the sample after 160 mT AF demagnetization step is still three orders of magnitude stronger than the moment of the sample holder used. The stereoplot shows that the directions of the medium and hard components are clustered together and this not significantly biasing the *REM* values.

The initial *REM* values (Fig. 4) of the studied samples are in the order of 10^{-2}, consistent with magnetite as main magnetic carrier of a *TRM* being imprinted by the geomagnetic field (*Wasilewski, 1977*; *Fuller et al., 1988*; *Kletetschka et al., 2004*). The *REM*(AF) curve shows generally stable values through the low and intermediate

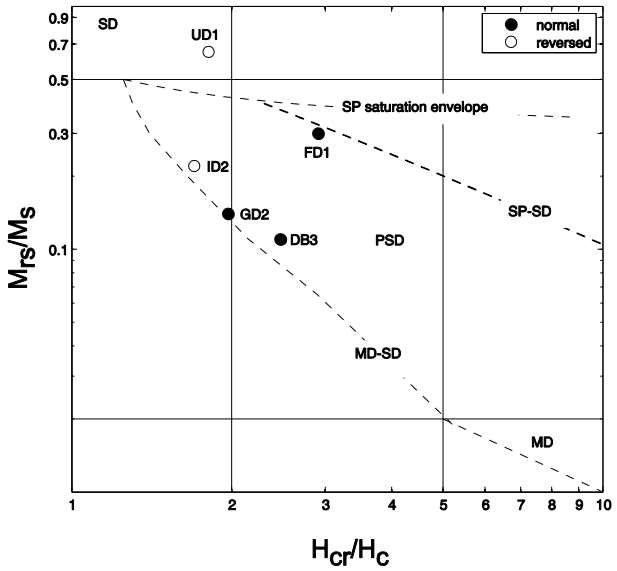

Fig. 2. The Day plot of the Gila diabase samples subjected to the study. Most of the samples show PSD like behavior or resemble the behavior of the MD-SD mixtures. M_{rs} - saturation remanent magnetization, M_S - saturation magnetization, H_{cr} - coercivity of remanence, H_C - coercive force. The solid lines are the boundaries after *Day et al. (1977)*, and the dashed lines are the mixing lines after *Dunlop (2002)*.

coercivity region up to the 25 – 40 mT AF field (Fig. 4 shows an example of this behavior for the FD1-2b) what is typical for MD magnetite bearing rocks (*Yu, 2006*; *Fuller et al., 1988*).

While demagnetizing the high coercivity component there is a significant increase in *REM* values observed. The *REM* gradually increases and stabilizes at ~0.5 in the 140 – 160 mT AF field region (Fig. 4). Such an increase (over one order of magnitude) is significantly higher than a similar effect attributed to the presence of SD or PSD grains described in *Yu (2006)*. Such behavior can be explained either by a presence of a low M_S (saturation magnetization) and high coercivity mineral (i.e. hematite; *Rochette et al., 2005*) or by the presence of the acicular SD magnetite grains which can easily acquire stable *NRM*, and due to the shape effect are magnetized with higher efficiency (*Kletetschka et al., 2004*).

In order to distinguish between those two possible carriers of the high coercivity and high efficiency component, the IRM acquisition curve measurement was selected as a most suitable indicator. The IRM acquisition curve was measured in three directions on the cylindrical specimen using the pulse magnetizer up to 3 T pulse field (Fig. 5). The results indicate that the material reaches saturation at the 200 mT field and the difference in *SIRM* level among three perpendicular directions is below 7%. The high coercivity minerals like hematite or pyrrhotite are saturating at much higher fields. In contrast

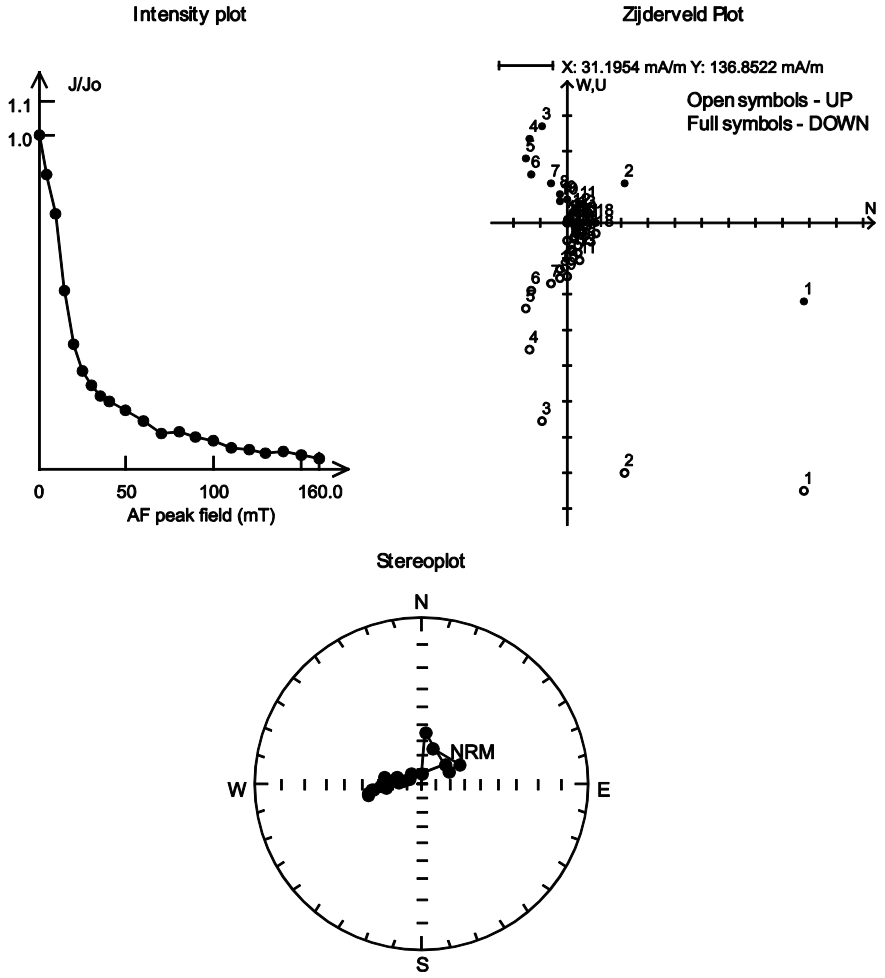

Fig. 3. The AF demagnetization plot of the *NRM* of the Gila diabase sample F1-2b. The intensity plot (top left) Zijderveld plot (top right) and stereoplot (bottom) are presented. Three main components (0 – 10 mT, 10 – 25 mT and 25 – 160 mT) can be identified. The stereoplot shows that the directions of the medium and hard components are clustered together. The directions are plotted in corrected geographical coordinates.

acicular magnetite grains are being saturated more easily than equi-dimensional ones. Thus the overall lack of remanence acquisition after 200 mT may indicate acicular magnetite grains to be the carriers of the high coercivity high *REM* component observed on the *REM*(AF) curve. The low scatter of the IRM anisotropy (below 7%) among three perpendicular directions shows the elongated axes of acicular magnetite grains not to be aligned. The presence of two distinct populations of magnetites is supported by the hysteresis parameters (Day Plot) and the thermomagnetic measurements.

3.2. Laboratory Shock Experiments with the Rowley Regis Basalt (UK)

Martelli and Newton (1977) used shaped charges to accelerate tips of an aluminum liner to impact a basalt block from Rowley Regis (UK) at velocities of approximately 15 km/s and described what they termed Shock Associated Remanent Magnetization (*SARM*). The term *SARM* is equal to *SRM* (Shock Remanent Magnetization) used in newer literature for the same phenomena. A low-frequency search coil showed that plasma was produced during the impact, causing local compression of the ambient magnetic field. They also demonstrated that a magnetic anomaly was generated at the crater margin and that magnetization was acquired by the basalt, which varied with the field strength. Mineralogical changes as a result of the impact were not detected, which is consistent with low pressure (1 – 2 GPa, see *Melosh, 1989*) and low temperature elevation (*French, 1998, Table 4.2*) near the crater rim and beyond. The only exception is the presence of a high pressure melt glass which was splashed onto the crater walls, containing projectile material. Such samples (coming from the crater proximity) containing melt glass ejecta were rejected from the magnetic studies.

Srnka et al. (1979) studied the variation of the intensity of magnetization and its AF demagnetization characteristics as a function of distance from the crater. The ambient field during the shock experiments was set to 1 mT and was perpendicular to the surface

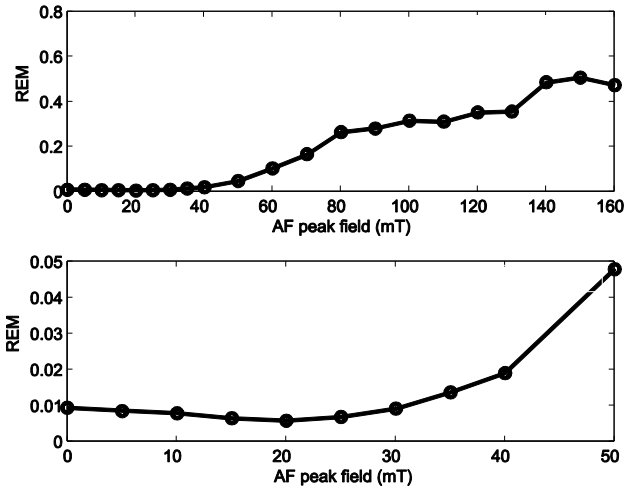

Fig. 4. The *REM*(AF) plot of the Gila diabase sample FD1-2B. The plot show REM values in the 0 – 160 mT AF demagnetization coercivity region (top) and detail for 0 – 50 mT region (bottom). The *REM* value in the low and medium coercivity region (up to 40 mT is roughly constant in the order of 10^{-2}. In the high coercivity region the *REM* value increases and stabilizes at *REM* value of 0.5. This behavior is interpreted as a contribution of two distinct populations of magnetic carriers (low to medium coercivity MD magnetite and high coercivity acicular SD magnetite).

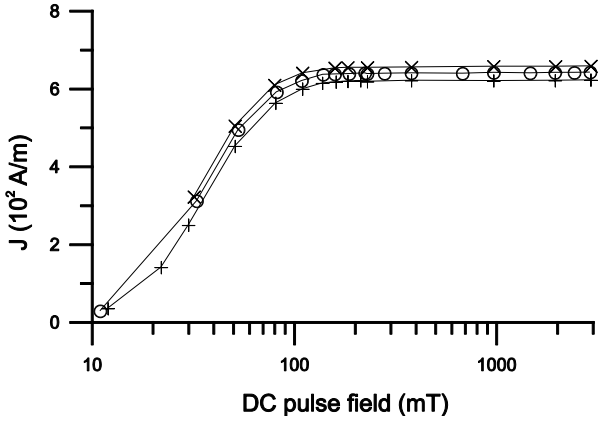

Fig. 5. The IRM acquisition curves up to 3 T of the sample FD1-2B form Gila diabase. The IRM acquisition was done along three perpendicular axes (*X*, *Y*, and *Z* correspond to sample coordinate system of the cylindrical specimen). The material saturates at 200 mT which is typical for the magnetite bearing rocks. There is no increase in saturation magnetization observed beyond this point ruling out the presence of hematite.

of the basalt block (parallel to the shooting direction). The results were recently re-analyzed in terms of the *REM*(AF) efficiency method.

Fig. 6 gives plots of *NRM* and *SIRM* (1 T field applied) versus the AF demagnetizing field for the control material and the samples at 4 and 20 cm from the center of the impact crater. There is a significant increase in magnetization (Fig. 6, top) from the value of 0.05 A/m (*NRM* of the control sample) towards 0.23 A/m (20 cm from crater) ending at 2.07 A/m (sample 4 cm from crater), which we interpret to be due to Shock Remanent Magnetization (*SRM*). In other words the material exhibits inverse dependence of magnetization upon distance from the center of the crater. There is a small increase in post shock *SIRM* at the shocked samples (Fig. 6, bottom) as the effect of the shock. The acquired shock remanence is predominantly soft, but also contains a component not demagnetized by 50 mT AF field.

In Fig. 7, the data are presented in the form of *REM*(AF) plots of *NRM* or *SRM* over *SIRM*. The control material shows plots reminiscent of altered basalts carrying secondary magnetization. The *REM* ratio at 20 mT is of order 10^{-3}, which is too low to be consistent with the *REM* ratio of a basalt carrying primary *TRM* acquired in geomagnetic field (*Fuller et al, 1988*). As seen in the sample 4 cm from the impact crater the shock produced different distribution of the AF demagnetization coercivity spectra compared to the *NRM* of unshocked samples.

The sample from 4 cm from the crater shows a decrease of SRM and *SIRM* during demagnetization, which is remarkably similar to the *TRM* behavior of magnetite in a strong field (higher *REM* values of 10^{-2} order and slightly increasing efficiency values through AF demagnetization process; *Fuller et al, 1988*). Yet, note that the mineralogical examination shows no evidence of significant residual heating.

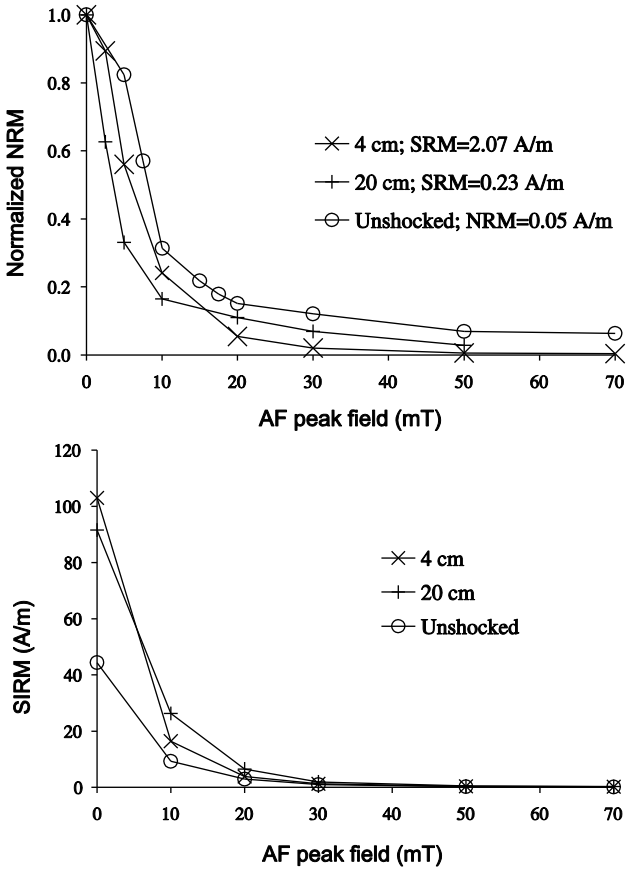

Fig. 6. AF demagnetization plots of *NRM* and *SRM* (top, normalized by initial value specified in the legend) and *SIRM* (bottom) of shocked and control samples from Rowley Regis basalt.

The sample from 20 cm from the crater has AF demagnetization characteristics somewhat intermediate between the control and the sample at 4 cm. The form of the curve is also consistent with secondary magnetization in basalts (*Fuller et al, 1988*).

4. CONCLUSIONS

The *REM*(AF) method can serve as fast tool to determine the origin of the *NRM* of the rocks.

In the case of Gila diabase the *REM*(AF) method proved useful, in combination with the IRM experiment, in identifying the carrier of the different *NRM* components. The low and medium coercivity components are carried by MD or PSD magnetite. The high coercivity ultra-stable *NRM* component is carried most likely by acicular magnetite. In such case, the need of determining the efficiency ratio throughout the whole AF

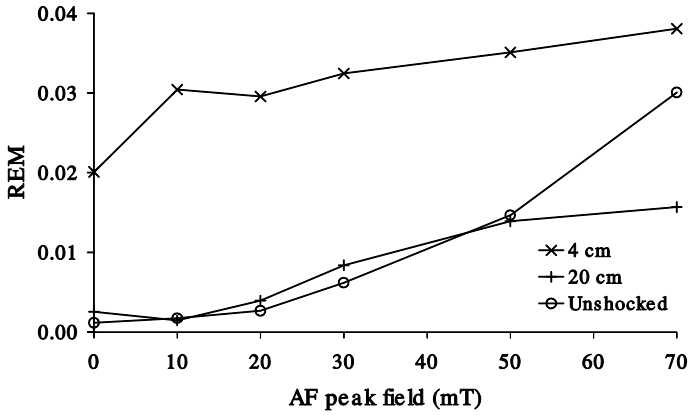

Fig. 7. *REM*(AF) plots of shocked and control samples from Rowley Regis basalt.

demagnetization sequence is obvious. The presence of two distinct populations of magnetite is further supported by the hysteresis parameters (Day Plot) and thermomagnetic analysis.

In the case of the shock experiments with the Rowley Regis basalt, the use of the *REM*(AF) plots makes clear that a strong *SRM* was acquired by the sample at 4 cm from the crater. This *SRM* has a distinct AF demagnetization coercivity spectra distribution compared to unshocked *NRM* and has similar AF demagnetization characteristics and coercivity distributions to those of a strong field *TRM*. Since this *SRM* was acquired well below the shock levels at which there is significant residual heating or mineralogical changes, the result may have bearing on the interpretation of the *NRM* of some extraterrestrial material that has been shocked to similar levels (e.g. magnetism of the Lunar rocks).

Acknowledgements: The authors would like to thank reviewers Simo Spassov and Ramon Egli for their constructive comments. This paper is SOEST contribution #7262 and HIGP contribution #1514.

References

Cisowski S.M., Dunn J.R., Fuller M. and Wasilewski P.J., 1990. NRM:IRM(s) demagnetization plots of intrusive rocks and the origin of their NRM. *Tectonophysics*, **184**, 35–54.

Cisowski S.M. and Fuller M., 1986. Lunar paleointensities via the IRMs normalization method and the early magnetic history of the Moon. In: Hartmann W.K., Phillips R.J. and Taylor G.J. (Eds.), *Origin of the Moon.* Lunar and Planetary Institute Houston, 411–424.

Day R., Fuller, M.D. and Schmidt V.A., 1977. Hysteresis properties of titano-magnetites: grain size and composition dependence. *Phys. Earth Planet. Inter.*, **13**, 260–266.

Dunlop D.J., 2002. Theory and application of the Day plot (Mrs/Ms versus Hcr/Hc). 2. Application to data for rocks, sediments and soils. *J. Geophys. Res.*, **107**, doi:10.1029/2001JB000487.

French B.M., 1998. Traces of Catastrophe: A Handbook of Shock-Metamorphic Effects in Terrestrial Meteorite Impact Structures. Technical Report, LPI-Contrib-954, Lunar and Planetary Institute, Houston, 120 pp.

Fuller M., Cisowski S., Hart M., Haston R. and Schmidtke E., 1988. NRM:IRM(s) demgnetization plots; an aid to the interpretation of natural remanent magnetization. *Geophys. Res. Lett.*, **15**, 518–521.

Fuller M., 1974. Lunar magnetism. *Rev. Geophys.*, **12**, 23–70.

Jarrard R.D. and Cockerham R.S., 1975. Reliability of paleolatitudes from Pacific DSDP sediment cores. *EOS Trans. Am. Geophys. Union*, **56**, 977–978.

Kletetschka G., Acuna M.H., Kohout T., Wasilewski P.J. and Connerney J.E.P., 2004. An empirical scaling law for acquisition of thermoremanent magnetization. *Earth Planet. Sci. Lett*., **226**, 521–528.

Martelli G. and Newton G., 1977. Hypervelocity cratering and impact magnetization of basalt. *Nature*, **269**, 478–480.

Melosh H.J., 1989. *Impact Cratering: A Geologic Process*. *Oxford Monographs on Geology and Geophysics No.11*, Oxford University Press, New York, Oxford, 245 pp.

Rochette P., Mathe P., Esteban L., Rakoto H., Bouchez J., Liu Q. and Torrent J., 2005. Non-saturation of the defect moment of goethite and fine-grained hematite up to 57 Teslas. *Geophys. Res. Lett.*, **32**, doi:10.1029/2005GL024196.

Srnka L.J., Martelli G., Newton G., Cisowski S.M., Fuller M. and Schaal R.B., 1979. Magnetic field and shock effects and remanent magnetization in a hypervelocity impact experiment. *Earth Planet. Sci. Lett.*, **42**, 127–137.

Yu Y.J. 2006. How accurately can NRM/SIRM determine the ancient planetary magnetic field intensity? *Earth Planet. Sci. Lett.*, **250**, 27–37.

Yu Y.J., Tauxe L. and Gee J.S., 2007. A linear field dependence of thermoremanence in low magnetic fields. *Phys. Earth Planet. Inter.*, **162**, 244–248.

Wasilewski P.J., 1977. Magnetic and microstructural properties of some lodestones. *Phys. Earth Planet. Inter.*, **15**, 349–362.